Altered pain responses in mice lacking α_{1E} subunit of the voltage-dependent Ca^{2+} channel

Hironao Saegusa*†, Takashi Kurihara*†, Shuqin Zong*, Osamu Minowa‡, An-a Kazuno*†, Wenhua Han*†, Yoshihiro Matsuda*†, Hitomi Yamanaka‡, Makoto Osanai*†, Tetsuo Noda‡§, and Tsutomu Tanabe*†¶

*Department of Pharmacology and Neurobiology, Graduate School of Medicine, Tokyo Medical and Dental University, and †CREST, Japan Science and Technology Corporation, 1-5-45 Yushima, Bunkyo-ku, Tokyo 113-8519, Japan; and ‡Department of Cell Biology, The Cancer Institute, Japanese Foundation for Cancer Research, 1-37-1 Kami-ikebukuro, Toshima-ku, Tokyo 170-8455, Japan

Communicated by Richard W. Tsien, Stanford University School of Medicine, Stanford, CA, March 20, 2000 (received for review December 21, 1999)

α_1 subunit of the voltage-dependent Ca^{2+} channel is essential for channel function and determines the functional specificity of various channel types. α_{1E} subunit was originally identified as a neuron-specific one, but the physiological function of the Ca^{2+} channel containing this subunit (α_{1E} Ca^{2+} channel) was not clear compared with other types of Ca^{2+} channels because of the limited availability of specific blockers. To clarify the physiological roles of the α_{1E} Ca^{2+} channel, we have generated α_{1E} mutant ($\alpha_{1E}-/-$) mice by gene targeting. The *lacZ* gene was inserted in-frame and used as a marker for α_{1E} subunit expression. $\alpha_{1E}-/-$ mice showed reduced spontaneous locomotor activities and signs of timidness, but other general behaviors were apparently normal. As involvement of α_{1E} in pain transmission was suggested by localization analyses with 5-bromo-4-chloro-3-indolyl β-D-galactopyranoside staining, we conducted several pain-related behavioral tests using the mutant mice. Although $\alpha_{1E}+/-$ and $\alpha_{1E}-/-$ mice exhibited normal pain behaviors against acute mechanical, thermal, and chemical stimuli, they both showed reduced responses to somatic inflammatory pain. $\alpha_{1E}+/-$ mice showed reduced response to visceral inflammatory pain, whereas $\alpha_{1E}-/-$ mice showed apparently normal response compared with that of wild-type mice. Furthermore, $\alpha_{1E}-/-$ mice that had been presensitized with a visceral noxious conditioning stimulus showed increased responses to a somatic inflammatory pain, in marked contrast with the wild-type mice in which long-lasting effects of descending antinociceptive pathway were predominant. These results suggest that the α_{1E} Ca^{2+} channel controls pain behaviors by both spinal and supraspinal mechanisms.

Voltage-dependent calcium channels (VDCCs) are classified into several distinct groups termed L-, N-, P-, Q-, R-, and T-types (1, 2). These types of VDCCs play important roles in various neuronal activities, including the control of neurotransmitter release, membrane excitability, and gene expression (3), but exact roles of each channel type are not necessarily clarified. In particular, functions of the R-type Ca^{2+} channel are least understood. The R-type Ca^{2+} channel was originally defined as a channel "Resistant" to blockers for L-, N-, P-, and Q-type Ca^{2+} channels (4); therefore, it is possible that the R-type current is a mixture of several different drug-resistant Ca^{2+} currents. Although the R-type Ca^{2+} channel is suggested to play a critical role in the release of neurotransmitters and somatodendritic excitability in a certain set of neurons (4–6), the physiological functions of this channel remain to be clarified.

VDCCs are heteromultimers composed of α_1, α_2-δ, β, and γ subunits. α_1 subunit is essential for channel function and determines the type of each Ca^{2+} channel. So far, 10 different α_1 cDNAs ($\alpha_{1A\text{-}I}$ and α_{1S}) have been cloned from a variety of tissues, and extensive studies have been made to clarify the relationship between each cloned α_1 subunit and native Ca^{2+} channels (2). Most of the α_1 subunits are known to have some molecular forms resulting from the alternative splicing, and, in most cases, the functional properties of each α_1 isoform have been confirmed to be analogous to those of the corresponding native channel. However, in the case of α_{1E} subunit, it is unclear whether Ca^{2+} channel containing the α_{1E} subunit (α_{1E} Ca^{2+} channel) represents only a single type of channel. There are several lines of evidence showing that the α_{1E} subunit, when expressed in heterologous systems, defines a mid-voltage activated channel where the voltage range of activation is between those of high-voltage and low-voltage activated channels (7, 8) with permeation properties similar to those of the T-type channels (9). Furthermore, expression of the α_{1E} gene corresponds to the presence of T-type channels in mouse spermatogenic cells and rat cardiac myocytes (10, 11). These results suggest that α_{1E} subunit underlies at least certain aspects of T-type Ca^{2+} channel functions. Nonetheless, expression of other members of the α_{1E} gene family produces high-voltage activated channels (12–15), and correlation between the neuronal rat α_{1E} gene expression and the neuronal R-type channel has been demonstrated (16), suggesting the involvement of α_{1E} subunit in high-voltage activated R-type channel.

To understand the physiological function of α_{1E} Ca^{2+} channel, a genetic approach instead of a pharmacological one seems quite useful. We have generated α_{1E} mutant mice by using homologous recombination in embryonic stem (ES) cells. Our strategy is to insert *lacZ* gene encoding β-galactosidase (β-gal) into the first exon of *cacna1e* encoding α_{1E} subunit to disrupt the gene and, at the same time, label the α_{1E}-expressing cells with the β-gal activity. Using this reporter gene, we have found that α_{1E} subunit is expressed in various regions involved in the control of pain transmission, such as dorsal root ganglia (DRGs) and dorsal horn of the spinal cord (SC). Recently, the modulation of Ca^{2+} channel function directly by channel blockers or indirectly through receptor/G-protein pathways (17) has attracted attention as a therapeutic means for controlling nociceptive transmission and soothing pain symptoms (18). Therefore, in this respect, to further investigate the physiological relevance of above-mentioned expression of α_{1E} Ca^{2+} channel in the pain-control system, we have also conducted several pain-related behavioral tests and found that the α_{1E} mutant mice show abnormalities in pain responses and that this mutant is useful for studying the mechanisms of pain transmission.

Materials and Methods

Gene Targeting. Genomic clones containing the mouse *cacna1e* were screened from the 129/Sv mouse genomic library (Strat-

Abbreviations: VDCC, voltage-dependent Ca^{2+} channel; DRG, dorsal root ganglion; ES, embryonic stem; SC, spinal cord; RM, nucleus raphe magnus; PAG, periaqueductal gray; β-gal, β-galactosidase; DIG, digoxigenin; RT, reverse transcription; X-Gal, 5-bromo-4-chloro-3-indolyl β-D-galactopyranoside; PGK, phosphoglycerate kinase; AP, alkaline phosphatase; PFA, paraformaldehyde; *PPT-A*, *preprotachykinin A*.

§Present address: Department of Molecular Genetics, Tohoku University, School of Medicine, 2-1 Seiryo-machi, Aoba-ku, Sendai 980-8575, Japan.

¶To whom reprint requests should be addressed. E-mail: t-tanabe.mphm@med.tmd.ac.jp.

The publication costs of this article were defrayed in part by page charge payment. This article must therefore be hereby marked "*advertisement*" in accordance with 18 U.S.C. §1734 solely to indicate this fact.

Article published online before print: *Proc. Natl. Acad. Sci. USA*, 10.1073/pnas.100124197. Article and publication date are at www.pnas.org/cgi/doi/10.1073/pnas.100124197

agene) with 184 bp (nucleotides 1–184) fragment from rabbit α_{1E} cDNA (19). Lambda phage clones containing the first exon were isolated, and the inserts were subcloned into pBluescriptII KS(+) (Stratagene).

Targeting vector BIIZneo was constructed by deleting a 2.3-kb fragment, located from the *Not*I site in the first exon to an *Sst*I site in the first intron, and inserting *nlacZ* (gene for *Escherichia coli* β-gal with a nuclear localization signal at its amino terminus) in-frame with the *cacna1e* reading frame and neomycin resistance gene driven by the phosphoglycerate kinase promoter (PGK-neo cassette) in its place. Thus, *nlacZ* and PGK-neo cassette is flanked by a 1.3-kb *Sal*I–*Not*I fragment (*Sal*I site is from the vector) and a 7-kb *Sst*I–*Sst*I fragment as 5′- and 3′-homologous regions, respectively. The diphtheria toxin A fragment gene was used as a negative selection marker (20).

Linearized BIIZneo was electroporated into J1 ES cells (derived from 129/Sv strain) (21), and homologous recombinant ES cells were screened by Southern blot analysis. Mutant mice were generated by using standard techniques (22). Mice with hybrid background of C57BL/6 (B_6) and 129/Sv were used in all of the experiments.

Southern and Northern Hybridization. Procedures were essentially the same as those reported previously (23), except that the probes were labeled with digoxigenin (DIG) by using DIG-High Prime (Roche Molecular Biochemicals) and that the labeled probe was detected by using alkaline phosphatase (AP)-labeled anti-DIG antibody and CSPD (disodium 3-(4-methoxyspiro{1,2-dioxetane-3, 2′-(5′-chloro)tricyclo[3.3.1.1^{3,7}]decan}-4-yl) phenyl phosphate, Roche Molecular Biochemicals) as a substrate for AP.

Reverse Transcription (RT)–PCR to Detect *cacna1e* Expression. Total RNA was prepared from mouse brains by the acid guanidinium thiocyanate-phenol-chloroform (AGPC) method (24) and used for the first-strand DNA synthesis with random hexamers and SuperscriptII (GIBCO/BRL). This cDNA preparation was treated with RNase H and used for the template for PCR (0.1 μg RNA equivalent was used in one reaction). PCR primers used were mA1E-F1(5′-AGCAGGAACCGACAAGGAACC-3′, corresponding to upstream region from the *nlacZ* insertion site in exon 1 of *cacna1e*) and mA1E-R1 (5′-GGTGGCCAGGATCATGTACTC-3′, possibly located in exon 2).

Immunoblotting. Immunoblotting was performed in a standard method. Briefly, a 100,000 × *g* membrane fraction from mouse brains was dissolved in SDS/PAGE sample buffer (10 mM Tris·HCl, pH 6.8, containing 0.005% Coomassie brilliant blue-G, 1.5% SDS, 2 M urea, and 10 mM DTT), and the proteins were resolved on a 5% polyacrylamide gel. The proteins were transferred onto polyvinylidene difluoride membrane (Immobilon P; Millipore), and the blot was probed with a rabbit polyclonal anti-α_{1E} antibody (Alomone Laboratories, Jerusalem) by using ECL system (Amersham Pharmacia).

Double Staining with 5-bromo-4-chloro-3-indolyl β-D-galactopyranoside (X-Gal) and IB4. DRGs and the SC were dissected out and immersion-fixed (or perfusion-fixed) in 4% paraformaldehyde (PFA)/PBS for 1 h, rinsed with PBS, and then stained with X-Gal overnight (25). They were then postfixed with 4% PFA in PBS. Paraffin or frozen sections (7 μm) were stained with peroxidase-labeled IB4 (Sigma) as described (26). As a substrate for peroxidase, 3,3′-diaminobenzidine was used.

X-Gal Staining Followed by RNA *in Situ* Hybridization. Frozen sections (7 μm) of DRGs stained with X-Gal were treated for *in situ* hybridization as described (27). A partial cDNA fragment (0.8 kb) of mouse *preprotachykinin A* (*PPT-A*), amplified by RT-PCR, was cloned into pCRII (Invitrogen), and the resultant plasmid was used as a template for synthesis of DIG-labeled riboprobes. Hybridized probe was detected by using AP-labeled anti-DIG antibody (Roche Molecular Biochemicals) with nitroblue tetrazolium chloride and 5-bromo-4-chloro-3-indolyl phosphate as substrates for AP. For cloning of the *PPT-A* cDNA fragment, primers SP-F1(5′-GTCTGACCGCAAAATCGAAC-3′, nucleotides 81–100, GenBank accession no. D17584) and SP-R1(5′-CAGGAAACATGCTGCTAGGA-3′ nucleotides 902–921) were used.

Behavioral Studies. The experiments were performed in a blind manner. The data were expressed as mean ± SEM and analyzed by Tukey test for multiple comparisons or by Student's *t* test for comparison between groups.

Anxiety-related tests. Mice of both sexes were used at the age of 6–9 wk (at the beginning of a series of experiments). All of the mice were tested sequentially in the three behavioral paradigms (see below). Mice were housed independently 1 wk before the start of the behavioral tests and were handled every day. Before starting each session, the test apparatus was cleaned with 1% acetic acid.

Open-field test. The open field was made of polyvinyl chloride (PVC) plates and was 50 cm × 50 cm × 40 cm in size. Each mouse was transferred to the center of the field, and its locomotor activity was measured for 5 min using a color tracking system (CompACT VAS; Muromachi Kikai, Tokyo).

Elevated plus-maze. The plus-maze consisted of two open arms (25 cm × 8 cm) and two closed arms with translucent plastic walls (15 cm high). The arms and the center square were made of white plastic (PVC) plates and placed at the 50-cm height from the floor. The open arms were surrounded by Plexiglas edges (3 mm high) to avoid animals' falling from the maze. Each mouse was transferred to the center square, and its behavior was videotaped for 5 min. The video images were captured as TIFF format data at 1 frame/s and analyzed on a Macintosh computer with NIH IMAGE EP 2.10 (O'Hara, Tokyo), a software modified from the NIH IMAGE program (developed at the U.S. National Institutes of Health and available at http://rsb.info.nih.gov/nih-image/). Total time spent on the open and closed arms was each calculated.

Startle response. Acoustic startle response was measured by using a startle chamber (SR-LAB System, San Diego). Briefly, each mouse was put into a Plexiglas cylinder, beneath which a piezoelectric accelerometer was attached to monitor the movement of the mouse. The mouse was exposed to a background noise (about 65 dB) for 5 min at the beginning of the session, and then acoustic stimuli (pulses of white noise with 105, 115, or 117 dB in a randomized order, each with 1 ms duration) were given from a speaker located 25 cm above the cylinder. The interval of the sound pulses was 30 s, and total of 60 pulses were given.

Pain-related tests. All of the experiments were conducted under the ethical guidelines for the study of experimental pain in conscious animals (28), and the protocol of the pain behavioral studies described in this paper has been approved by the Animal Care Committee of Tokyo Medical and Dental University. Mice of both sexes were used at the age of 15–20 wk. All of the mice had been used for the above-mentioned behavioral tests before the pain-related tests were performed. Mice were acclimatized to the experimental room, which is sound-proof, for at least 1 h before the experiments. The experiments were performed in the light phase (L:D = 12:12).

Von Frey test. Fifty percent hindpaw withdrawal threshold to mechanical stimulation was determined with calibrated von Frey hairs using the up–down paradigm (29).

Paw flick test. Hindpaw withdrawal latency was measured by the method of Hargreaves (30) using a Ugo Basile plantar test apparatus. The tests were performed at low (infrared intensity

10) and high (infrared intensity 40) intensities. The cut-off time was 23 s for both intensities.

Tail flick test. Two-thirds of the tail was immersed in heated water (48–49°C), with the mouse lightly restrained, and the latency to flick the tail was recorded. The cut-off time was 25 s.

Hot plate test. Hot plate tests were performed at three different temperatures (50, 52, and 55°C). Latency to lick the hindpaw was recorded. The cut-off time was 60 s for 50°C, 40 s for 52°C, and 30 s for 55°C.

Formalin test. Under light halothane anesthesia, formalin (10 μl of 0.5% PFA in saline) was injected s.c. into the dorsal surface of a hindpaw. Then the mouse was transferred to an observation chamber. The time spent in licking or biting the injected paw was recorded at 1–3 min and 5–7 min after injection (phase 1) and then for 2 min every 5 min during 10–47 min after injection (phase 2).

Writhing test. Acetic acid (0.6%) was injected i.p. (0.1 ml/10 g body weight), and the number of writhes was counted for 20 min.

Peripheral inflammatory response. The extent of peripheral inflammation was assessed by measuring the volume of the right PFA-injected (V_r) and the left control (V_l) hindpaws with plethysmometer (Unicom TK101; Unicom, Chiba, Japan). Percent peripheral inflammation was calculated as follows: % peripheral inflammation = $(V_r - V_l)/V_l \times 100$.

Results and Discussion

Generation of α_{1E} Ca^{2+} Channel Mutant Mice. In the targeting construct (BIIZneo), *nlacZ* was fused in-frame to the coding sequence of *cacna1e* gene (Fig. 1*A*). Thus, the *nlacZ* insertion is expected to disrupt the *cacna1e* gene and to make it possible to mark the α_{1E}-expressing cells by the β-gal activity. We introduced linearized BIIZneo into J1 ES cells and screened for targeted ES cells. A total of 3 of 127 clones were found to be correctly targeted, and one of them yielded germ-line chimeras (Fig. 1*B*). Homozygous mutants ($\alpha_{1E}-/-$), obtained by intercrossing heterozygotes ($\alpha_{1E}+/-$), were viable and fertile. In both RT-PCR and Northern blot analyses of brain RNA, no positive signals were observed in the samples from $\alpha_{1E}-/-$ (Fig. 1 *C* and *D*), nor was detected the α_{1E} protein by the immunoblot analysis of brain membrane proteins from the $\alpha_{1E}-/-$ mice (Fig. 1*E*). Thus, we conclude that this targeted *nlacZ* insertion resulted in a null mutation for *cacna1e*.

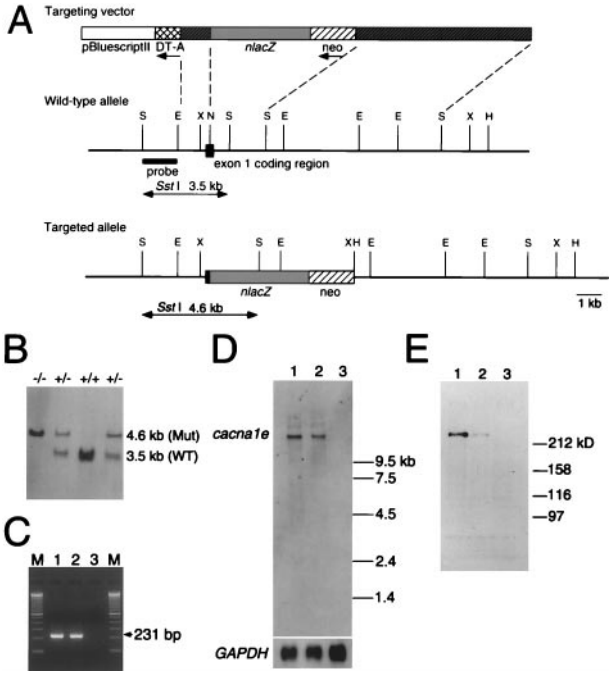

Fig. 1. Generation of α_{1E}-deficient mice. (*A*) Simplified restriction map around exon 1 of *cacna1e* gene and structure of the targeting vector. Coding region of exon 1 is boxed. neo, PGK-neo cassette; DT-A, diphtheria toxin-A fragment gene; E, *Eco*RI; N, *Not*I; S, *Sst*I; X, *Xba*I. (*B*) Southern blot analysis of tail DNA. DNA was digested with *Sst*I, and the blot was hybridized with a probe shown in *A*. The 3.5-kb band is derived from the wild-type allele (WT) and the 4.6-kb band from the targeted allele (Mut). +/+, wild-type; +/−, heterozygote; −/−, homozygous mutant. (*C*) RT-PCR analysis. cDNA derived from brain total RNA was used as a template. A fragment of 231 bp is diagnostic of *cacna1e* expression. M, 100 bp ladder (GIBCO/BRL). (*D*) Northern blot analysis. Poly(A)$^+$ RNA (2.5 μg) from mouse brains was loaded in each lane. The blot was probed with a *cacna1e* cDNA fragment (about 1 kb) corresponding to cytoplasmic loop between the repeat II and III of α_{1E}. *GAPDH* probe was used for loading control (35). (*E*) Immunoblot analysis. Brain membrane proteins (100 μg/lane) were probed with a rabbit polyclonal anti-α_{1E} antibody. This antibody detects a single band with molecular mass of *ca.* 250 kDa. Lane 1, wild-type; lane 2, heterozygote; lane 3, homozygous mutant in *C*, *D*, and *E*.

Abnormal Fear in the Homozygous Mutant Mice. $\alpha_{1E}-/-$ mice often seemed to struggle for escape more vigorously than wild-type ($\alpha_{1E}+/+$) mice, when an experimenter tried to pick them up. This might suggest the animals' abnormal emotional state, and, therefore, we tested them in several anxiety-related behavioral paradigms. Although it seemed that the behaviors of $\alpha_{1E}-/-$ mice were grossly normal, they showed a significantly reduced level of spontaneous locomotor activities compared with $\alpha_{1E}+/+$ mice as revealed by an open-field test (Fig. 2 *A* and *B*). The percentage of the time spent in the center region of the field was also significantly lower in the $\alpha_{1E}-/-$ mice (Fig. 2 *C* and *D*). These observations suggest that $\alpha_{1E}-/-$ mice have an increased level of anxiety. We further examined the level of the fear that is assessed by the elevated plus-maze and startle response tests. In both tests, however, no significant differences were observed among the three genotypes (Fig. 2 *E* and *F*). These results suggest that the $\alpha_{1E}-/-$ mice show increased level of fear for some kind of stimuli such as exposure to a novel environment.

α_{1E} Ca^{2+} Channel Is Expressed in Various Regions Involved in the Control of Pain Transmission. We examined the expression of α_{1E} Ca^{2+} channel in the SC and DRGs by assessing the β-gal activity. When a whole SC from an $\alpha_{1E}+/-$ mouse was stained with X-Gal, dense staining was observed in the dorsal horn along the entire length of the SC (Fig. 3 *A* and *B*). To examine the nature of the cells expressing β-gal, the X-Gal-stained SC was sectioned and double-labeled with an anti-substance P antibody (data not shown) or with a plant lectin IB4. It is generally accepted that primary afferent nociceptive neurons are roughly classified into two types: one produces peptide neurotransmitters such as substance P or calcitonin-gene-related peptide and the other expresses some enzymatic markers and binds IB4 (31). The results of double-staining show that α_{1E}-expressing cells in the SC are located in the laminae I, II, and possibly III, because the X-Gal signals were observed both outside and inside the IB4 signals (Fig. 3*C*). Therefore, at least a part of the dorsal horn neurons expressing α_{1E} are thought to be innervated by primary afferent nociceptive neurons.

In the DRGs from $\alpha_{1E}+/-$ mice, some neurons expressed β-gal (Fig. 3*D*). To determine what types of cells expressed α_{1E}, X-Gal-stained lumbar DRG sections were labeled with IB4 or *in situ* hybridized with an antisense *PPT-A* (encoding substance P) riboprobe. The results show that some X-Gal-stained neurons were positive for both (Fig. 3 *E* and *F*). Thus, α_{1E} is expressed in both categories of primary afferent neurons.

α_{1E} Mutant Mice Behave Normally Against Acute Pain Stimuli. The above-mentioned results raise a possibility that α_{1E} Ca^{2+} channel is involved in pain transmission. We therefore analyzed pain-

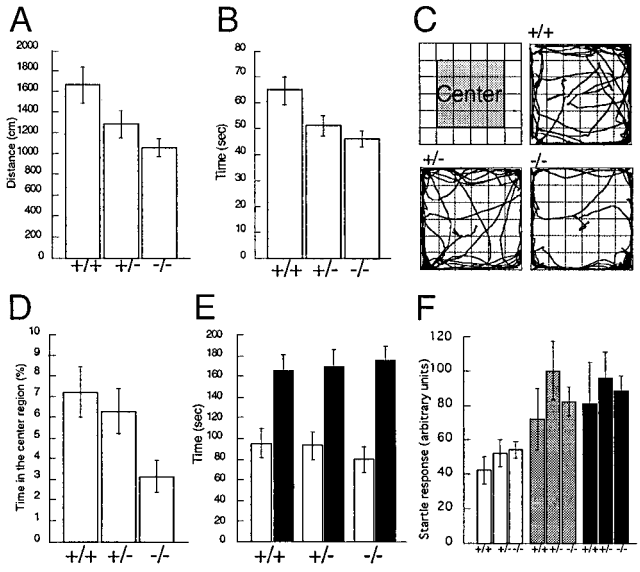

Fig. 2. Anxiety-related behavioral tests of wild-type (+/+), heterozygote (+/−), and homozygous mutant mice (−/−). (*A* and *B*) An open-field test for a total of 5 min shows significant differences in path length (*A*) and locomotion time (*B*) in −/−mice ($P < 0.05$ and $P < 0.01$, respectively). +/+, $n = 14$; +/−, $n = 22$; −/−, $n = 20$. (*C*) Criteria for center vs. border. The center was defined as the inner 16 squares (*C*, *Upper Left*). An example of walking paths of a +/+ mouse (*Upper Right*), a +/− mouse (*Bottom Left*), and a −/− mouse (*Bottom Right*) in open-field tests. (*D*) Percentage of the time spent in the center for a total of 5 min in the open-field test shows a significant difference in −/− mice ($P < 0.05$). +/+, $n = 14$; +/−, $n = 22$; −/−, $n = 20$. (*E*) Elevated plus-maze test. Open columns, time spent on open arms; filled columns, time spent on closed arms. No statistically significant difference was observed among the genotypes. +/+, $n = 15$; +/−, $n = 18$; −/−, $n = 19$. (*F*) Startle responses against various intensities of sound pulses. Stimuli with 105 dB (open columns), 115 dB (gray columns), and 117 dB (filled columns) were given. No statistically significant difference was observed among the genotypes. +/+, $n = 8$; +/−, $n = 10$; −/−, $n = 15$.

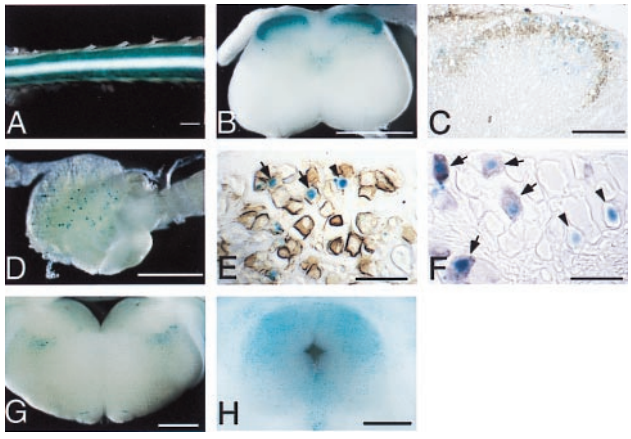

Fig. 3. *cacna1e* expression in the nervous system involved in pain transmission. (*A* and *B*) X-Gal staining (blue) of the whole SC from a heterozygous mutant. (*A*) Dorsal view. (*B*) Cross-section. (*C*) IB4 binding (brown signal) was assessed in an X-Gal-stained SC section from a heterozygous mutant. (*D*) Whole lumbar DRG was stained with X-Gal. (*E* and *F*) X-Gal-stained lumbar DRG neurons were further stained with molecular markers. (*E*) Staining with IB4. Some of the X-Gal-stained neurons are also stained with IB4 (arrows). (*F*) RNA *in situ* hybridization with an antisense *PPT-A* riboprobe. Some of the X-Gal-positive neurons show *PPT-A* signal (arrows). Neurons labeled with only X-Gal were shown by arrowheads in *E* and *F*. (*G*) X-Gal staining of RVM from a heterozygous mutant. Staining was not observed in the RM. (*H*) X-Gal staining of PAG from a heterozygous mutant. (Scale bars: 1 mm in *A*, *B*, and *G*; 0.5 mm in *D* and *H*; 100 μm in *C*; 50 μm in *E* and *F*.) *In situ* hybridization experiments of wild-type mouse brain sections using DIG-labeled *cacna1e* riboprobes were in good agreement with those obtained by X-Gal staining of the heterozygous mutant brain, suggesting the X-Gal staining reflects the expression of *cacna1e* gene (data not shown).

related behaviors of the α_{1E} mutant mice. First, threshold for mechanical stimuli was determined by von Frey test, but animals of each genotype exhibited no significant difference in the threshold (Fig. 4*A*). Then, we examined responses to noxious thermal stimuli by paw flick, tail flick, and hot plate tests. The paw flick and tail flick tests were used to evaluate the spinal reflexes at the lumbar and sacral levels, respectively, and the hot plate test was to examine a supraspinal involvement in nociception (32). Again, no significant differences among genotypes were detected by these assays (Fig. 4 *B–D*). Thus, the responses to acute mechanical or noxious thermal stimuli are normal in the α_{1E} mutant mice.

Altered Responses Against Noxious Inflammatory Stimuli in α_{1E} Mutant Mice. We next examined the responses related to the inflammatory pain by the formalin test and the acetic acid writhing test. Injection of formalin into a mouse hindpaw elicits a biphasic pain-response. In phase 1, formalin directly stimulates nociceptors and induces the pain response, and, in phase 2, inflammation caused by formalin elicits the pain response (33). We injected formalin into a hindpaw and observed the mouse behavior. In phase 1, no significant difference was observed between the α_{1E}+/+ and mutant mice. However, the phase 2 response was significantly lowered in the α_{1E}+/− and α_{1E}−/− mice (Fig. 5*A*). Thus, α_{1E} Ca^{2+} channel in SC and/or DRG is responsible for transmitting the inflammatory pain sensation (Fig. 6), suggesting that blockers of this channel may be useful for antinociception.

Intraperitoneal injection with acetic acid induces a typical behavior termed writhing, which is a model for a visceral pain with inflammation (33). Interestingly, the writhing response

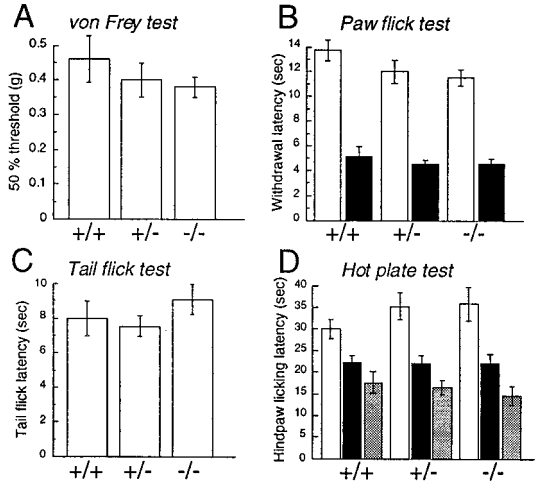

Fig. 4. Acute nociceptive responses of wild-type(+/+), heterozygote (+/−), and homozygous mutant mice (−/−). (*A*) Fifty percent hindpaw withdrawal thresholds to stimulation with von Frey hairs (+/+, $n = 13$; +/−, $n = 21$; −/−, $n = 24$). (*B*) Hindpaw withdrawal latencies to noxious thermal stimuli with a low intensity (open columns) and a high intensity (filled columns). +/+, $n = 13$, 12; +/−, $n = 21$, 16; −/−, $n = 24$, 15 at low and high intensities, respectively. (*C*) Tail flick latencies to noxious heat (48–49°C; +/+, $n = 12$; +/−, $n = 17$; −/−, $n = 15$). (*D*) Hindpaw licking latencies in the hot plate tests (+/+, $n = 11$; +/−, $n = 17$; −/−, $n = 15$) at 50 °C (open columns), 52 °C (filled columns), and 55 °C (gray columns). There are no significant differences in these four tests across the three genotypes.

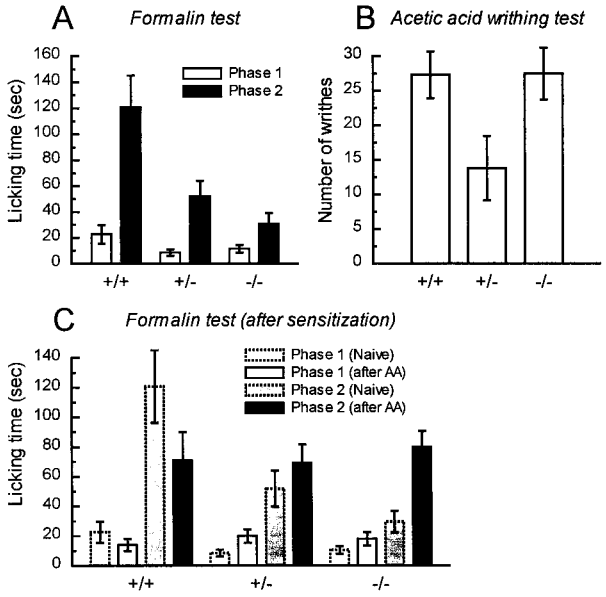

Fig. 5. Nociceptive responses to noxious chemical stimulation of cutaneous or visceral tissue. (*A*) Formalin-evoked hindpaw-licking behavior in wild-type (+/+), heterozygote (+/−), and homozygous mutant mice (−/−). Open columns represent phase 1 (1–7 min after injection); filled columns, phase 2 (10–47 min after injection). Phase 2 responses were significantly reduced in hetero- and homozygous mutant mice ($P < 0.01$ and $P < 0.001$, respectively). +/+, $n = 8$; +/−, $n = 7$; −/−, $n = 9$. We found no difference in the peripheral inflammatory response to formalin injection [% peripheral inflammation in +/+ and −/− mice were 30.0 ± 5.3 ($n = 7$) and 29.8 ± 3.9 ($n = 5$), respectively]. (*B*) Visceral nociceptive response (abdominal writhes) produced by i.p. injection of 0.6% acetic acid (+/+, $n = 6$; +/−, $n = 8$; −/−, $n = 13$). Only heterozygous mutant mice exhibited reduced responses ($P < 0.05$). (*C*) Effects of sensitization by a noxious visceral conditioning stimulus on the formalin-evoked somatic nociception. In wild-type mice, which had received a noxious visceral stimulus (0.6% acetic acid, AA) 18–20 days before, the phase 2 response (filled column) was considerably reduced compared with the control (gray column). In a separate set of experiments, we also observed significantly reduced phase 2 responses ($P < 0.001$) in the sensitized B6 mice compared with the naive counterpart ($n = 26$ and $n = 25$, respectively). The phase 2 response in homozygous mutant mice after sensitization was significantly facilitated ($P < 0.01$) compared with that of naive homozygous mutants. +/+, $n = 4$; +/−, $n = 10$; −/−, $n = 10$. Data of naive mice (columns with dotted lines) are presented for comparison.

after administration of 0.6% acetic acid was significantly decreased only in the α_{1E}+/− mice (Fig. 5*B*). This suggests that the decrease in the density of α_{1E} Ca^{2+} channel (to about half of the normal level) is responsible for lowering pain sensation caused by inflammation. This also raises a possibility that other channels compensate for the loss of α_{1E} in the α_{1E}−/− mice. It may be worth noting here that the response to formalin of the α_{1E}−/− mice was smaller than that in the α_{1E}+/+, in contrast with the case of the acetic acid writhing test. This difference in the responses of α_{1E}−/− mice in both tests may reflect the different routes of entry of the inflammatory nociception: pain signals produced by formalin enter the lumbar SC, whereas those produced by acetic acid enter the thoracic and lumbar SC. If a compensatory mechanism occurred in the α_{1E}−/− mice, it would have been at the thoracic level. Taking this into consideration, we studied the expression of genes coding for α_{1A}, α_{1B}, α_{1C}, α_{1D}, and α_{1G} subunits of the VDCCs in the thoracic and lumbar SC by semiquantitative RT-PCR. Expression of these genes, however, did not significantly differ in both regions among α_{1E}+/+, α_{1E}+/−, and α_{1E}−/− mice (data not shown). So far, we have not obtained data indicating the presence of a compensatory mechanism. Although these lines of evidence do not

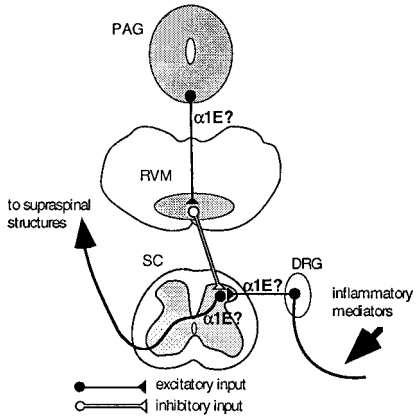

Fig. 6. A model for explaining α_{1E} mutant phenotypes. Inflammatory mediators produced as a result of a chemical irritant injection stimulate primary afferent fibers, leading to excitation of the dorsal horn neurons. This information is further conveyed to supraspinal structures (e.g., thalamus). α_{1E} Ca^{2+} channel mediates either or both of these sensory transmissions in a gene-dosage-dependent manner. α_{1E} Ca^{2+} channel also mediates the descending antinociceptive signal by increasing the excitability of PAG neurons and/or by eliciting the release of an excitatory transmitter(s) from the terminals, which activate RM neurons. Serotonin released by the RM neurons in turn exerts inhibitory control on the spinal pain transmission.

automatically eliminate the possibility of the presence of compensatory mechanism, we rather prefer to propose that the writhing response in the α_{1E}−/− mice was apparently maintained because of a blockade of the supraspinal antinociceptive pathway. In fact, the following findings support this possibility.

Effects of Visceral Noxious Conditioning Stimuli on the Following Somatic Nociceptive Response. We first challenged the mice with acetic acid to sensitize them. The pain responses were terminated about 1 h after acetic acid injection. Then, we returned the mice to the home cage. Behaviors of the mice were apparently normal, and they did not show any signs of pain. The sensitized mice were further housed for 18–20 days and then injected a hindpaw with formalin. The response to formalin in phase 1 is slightly reduced in the α_{1E}+/+ mice, whereas it is slightly enhanced in the α_{1E}+/− and the α_{1E}−/− mice. On the other hand, a marked contrast was observed in the phase 2 response in the α_{1E}+/+ and α_{1E}−/− mice (Fig. 5*C*). In α_{1E}−/− mice, the phase 2 response was significantly increased as compared with that of naive α_{1E}−/− mice injected with formalin, whereas α_{1E}+/+ mice exhibited an opposite response. The apparent hypoalgesic effect observed in the α_{1E}+/+ mice can be interpreted as an example of descending antinociceptive regulatory mechanism. This descending antinociceptive pathway is somewhat similar but is different from the diffuse noxious inhibitory control pathway (34). We have recently identified that this suppression of pain response in sensitized B_6 mice is opioid-independent but sensitive to serotonin receptor (5-$HT_{2A/2C}$) antagonists,‖ suggesting serotonergic involvement in this descending antinociceptive pathway. The increased pain response observed in the α_{1E}−/− mice would be explained by the attenuation of the inhibitory effect of descending antinociceptive pathway and unimpaired activation of the descending nociceptive facilitatory pathway. Indeed, similar kind of stimuli are known to activate both antinociceptive and nociceptive pathways at the supraspinal level (36).

Primary origin of the serotonergic neurons involved in the

‖Kurihara, T., Nonaka, T. & Tanabe, T. (2000) *Jpn. J. Pharmacol.* **82,** Suppl. 1, 163 (abstr.).

descending inhibitory pathway is thought to be the nucleus raphe magnus (RM) located in the rostral ventromedial medulla (RVM) (37). However, X-Gal staining of the $\alpha_{1E}+/-$ brains did not reveal α_{1E} expression in the RM (Fig. 3*G*), but was detected in the periaqueductal gray (PAG) (Fig. 3*H*), which is suggested to control the activity of RM neurons (37). Thus, it is interesting to speculate that α_{1E} Ca^{2+} channel is responsible for the descending antinociception by controlling the excitability of PAG neurons and/or by releasing an excitatory transmitter(s) from them to activate RM neurons (Fig. 6), although further rigorous research would be necessary to prove this hypothesis.

Results of our recent study suggest that the prolonged activation of the antinociceptive pathway is not evoked by a pretreatment with formalin injection in contrast with the acetic acid injection.[‖] This would be compatible with the lowered response in the formalin test (Fig. 5*A*) and enhanced response (compared with the $\alpha_{1E}+/-$ mice) in the acetic acid writhing test in the naive $\alpha_{1E}-/-$ mice (Fig. 5*B*). The activation of the antinociceptive pathway elicited by acetic acid lasts for a surprisingly long term (at least 3 wk, so far examined). It may be interesting to study whether this long-term effect is accompanied by neuronal plasticity such as long-term potentiation of synaptic transmission (38) at the PAG/RM axis. If it is, Ca^{2+} entering through α_{1E} Ca^{2+} channel must be critical for the process.

To date, there have been several reports on genetically engineered mice that exhibit deficits in pain-related phenomena (reviewed in ref. 39). As far as we know, however, our α_{1E} mutant mice are unique in that they show the possibility of the deficits in the descending antinociceptive pathway. Thus, they provide an intriguing clue to elucidate antinociceptive mechanism which is important to the animal's defensive system.

We thank S. Inada, M. Kondoh, T. Muno, M. Tamura, N. Yoneda, L. Gunsten, C. Le, and staff at Animal Research Center of Tokyo Medical and Dental University for assistance, Y. Kiyama and Prof. M. Mishina for helpful advice in behavioral tests, and Dr. T. Murakoshi for critically reading the manuscript. This work was supported by grants from the Ministry of Health and Welfare, the Ministry of Education, Science, Sports and Culture, Japan, Uehara Memorial Foundation, and Naito Memorial Foundation.

1. Catterall, W. A. (1998) *Cell Calcium* **24,** 307–323.
2. Hofmann, F., Lacinova, L. & Klugbauer, N. (1999) *Rev. Physiol. Biochem. Pharmacol.* **139,** 33–87.
3. Berridge, M. J. (1998) *Neuron* **21,** 13–26.
4. Zhang, J.-F., Randall, A. D., Ellinor, P. T., Horne, W. A., Sather, W. A., Tanabe, T., Schwarz, T. L. & Tsien, R. W. (1993) *Neuropharmacology* **32,** 1075–1088.
5. Wu, L.-G., Borst, G. G. & Sakmann, B. (1998) *Proc. Natl. Acad. Sci. USA* **95,** 4720–4725.
6. Wu, L.-G., Westenbroek, R. E., Borst, J. G. G., Catterall, W. A. & Sakmann, B. (1999) *J. Neurosci.* **19,** 726–736.
7. Soong, T. W., Stea, A., Hodson, C. D., Dubel, S. J., Vincent, S. R. & Snutch, T. P. (1993) *Science* **260,** 1133–1136.
8. Stephens, G. J., Page, K. M., Burley, J. R., Berrow, N. S. & Dolphin, A. C. (1997) *Pflügers Arch.* **433,** 523–532.
9. Bourinet, E., Zamponi, G. W., Stea, A., Soong, T. W., Lewis, B. A., Jones, L. P., Yue, D. T. & Snutch, T. P. (1996) *J. Neurosci.* **16,** 4983–4993.
10. Liévano, A., Santi, C. M., Serrano, C. J., Trevño, C. L., Bellve, A. R., Hernández-Cruz, A. & Darszon, A. (1996) *FEBS Lett.* **388,** 150–154.
11. Piedras-Rentería, E. S., Chen, C. C. & Best, P. M. (1997) *Proc. Natl. Acad. Sci. USA* **94,** 14936–14941.
12. Ellinor, P. T., Zhang, J.-F., Randall, A. D., Zhou, M., Schwarz, T. L., Tsien, R. W. & Horne, W. A. (1993) *Nature (London)* **363,** 455–458.
13. Williams, M. E., Marubio, L. M., Deal, C. R., Hans, M., Brust, P. F., Philipson, L. H., Miller, R. J., Johnson, E. C., Harpold, M. M. & Ellis, S. B. (1994) *J. Biol. Chem.* **269,** 22347–22357.
14. Schneider, T., Wei, X., Olcese, R., Costantin, J. L., Neely, A., Palade, P., Perez-Reyes, E., Qin, N., Zhou, J., Crawford, G. D., *et al.* (1994) *Recept. Channels* **2,** 255–270.
15. Wakamori, M., Niidome, T., Furutama, D., Furuichi, T., Mikoshiba, K., Fujita, Y., Tanaka, I., Katayama, K., Yatani, A., Schwartz, A. & Mori, Y. (1994) *Recept. Channels* **2,** 303–314.
16. Piedras-Rentería, E. S. & Tsien, R. W. (1998) *Proc. Natl. Acad. Sci. USA* **95,** 7760–7765.
17. Zamponi, G. W. & Snutch, T. P. (1998) *Curr. Opin. Neurobiol.* **8,** 351–356.
18. Yaksh, T. L. (1999) *Trends Pharmacol. Sci.* **20,** 329–337.
19. Niidome, T., Kim, M. S., Friedrich, T. & Mori, Y. (1992) *FEBS Lett.* **308,** 7–13.
20. Yagi, T., Ikawa, Y., Yoshida, K., Shigetani, Y., Takeda, N., Mabuchi, I., Yamamoto, T. & Aizawa, S. (1990) *Proc. Natl. Acad. Sci. USA* **87,** 9918–9922.
21. Li, E., Bestor, T. H. & Jaenisch, R. (1992) *Cell* **69,** 915–926.
22. Papaioannou, V. & Johnson, R. (1993) in *Gene Targeting: A Practical Approach*, ed. Joyner, A. L. (IRL, Oxford), pp. 107–146.
23. Saegusa, H., Takahashi, N., Noguchi, S. & Suemori, H. (1996) *Dev. Biol.* **174,** 55–64.
24. Chomczynski, P. & Sacchi, N. (1987) *Anal. Biochem.* **167,** 156–159.
25. Minabe-Saegusa, C., Saegusa, H., Tsukahara, M. & Noguchi, S. (1998) *Dev. Growth Differ.* **40,** 343–353.
26. Streit, W. J. (1990) *J. Histochem. Cytochem.* **38,** 1683–1686.
27. Wilkinson, D. G. & Nieto, M. A. (1993) in *Guide to Techniques in Mouse Development*, eds. Wassarman, P. M. & DePamphilis, M. L. (Academic, San Diego), pp. 368–370.
28. International Association for the Study of Pain (1995) in *Core Curriculum for Professional Education in Pain*, ed. Fields, H. L. (IASP, Seattle), 2nd Ed., pp. 111–112.
29. Chaplan, S. R., Bach, F. W., Pogrel, J. W., Chung, J. M. & Yaksh, T. L. (1994) *J. Neurosci. Methods* **53,** 55–63.
30. Hargreaves, K., Dubner, R., Brown, F., Flores, C. & Joris, J. (1988) *Pain* **32,** 77–88.
31. Snider, W. D. & McMahon, S. B. (1998) *Neuron* **20,** 629–632.
32. Chapman, C. R., Casey, K. L., Dubner, R., Foley, K. M., Gracely, R. H. & Reading, A. E. (1985) *Pain* **22,** 1–31.
33. Tjølsen, T. & Hole, K. (1997) in *The Pharmacology of Pain,* eds. Dickenson, A. & Besson, J.-M. (Springer, Berlin), pp. 1–20.
34. Villanueva, L. & Le Bars, D. (1995) *Biol. Res.* **28,** 113–125.
35. Sabath, D. E., Broome, H. E. & Prystowsky, M. B. (1990) *Gene* **91,** 185–191.
36. Coutinho, S. V., Urban, M. O. & Gebhart, G. F. (1998) *Pain* **78,** 59–69.
37. Fields, H. L. & Basbaum, A. I. (1994) in *Textbook of Pain*, eds. Wall, P. D. & Melzack, R. (Churchill Livingstone, Edinburgh), 3rd Ed., pp. 243–257.
38. Bliss, T. V. P. & Collingridge, G. L. (1993) *Nature (London)* **361,** 31–39.
39. Mogil, J. S. & Grisel, J. E. (1998) *Pain* **77,** 107–128.